Hierarchical Protein Folding: Asymmetric Unfolding of an Insulin Analogue Lacking the A7−B7 Interchain Disulfide Bridge†

Qing-Xin Hua,‡ Satoe H. Nakagawa,§ Wenhua Jia,‡ Shi-Quan Hu,|| Ying-Chi Chu,|| Panayotis G. Katsoyannis,*,|| and Michael A. Weiss*,‡

Department of Biochemistry, Case Western Reserve University School of Medicine, Cleveland, Ohio 44016, Department of Biochemistry and Molecular Biology, The University of Chicago, Chicago, Illinois 60637, and Department of Biochemistry and Molecular Biology, Mount Sinai School of Medicine of New York University, New York, New York 10029

Received May 18, 2001; Revised Manuscript Received August 13, 2001

ABSTRACT: The landscape paradigm of protein folding can enable preferred pathways on a funnel-like energy surface. Hierarchical preferences may be manifest as a nonrandom pathway of disulfide pairing. Stepwise stabilization of structural subdomains among on-pathway intermediates is proposed to underlie the disulfide pathway of proinsulin and related molecules. Here, effects of pairwise serine substitution of insulin's exposed interchain disulfide bridge (Cys^{A7}−Cys^{B7}) are characterized as a model of a late intermediate. Untethering cystine A7−B7 in an engineered monomer causes significantly more marked decreases in the thermodynamic stability and extent of folding than occur on pairwise substitution of internal cystine A6−A11 [Weiss, M. A., Hua, Q. X., Jia, W., Chu, Y. C., Wang, R. Y., and Katsoyannis, P. G. (2000) *Biochemistry 39*, 15429−15440]. Although substantially disordered and without significant biological activity, the untethered analogue contains a molten subdomain comprising cystine A20−B19 and a native-like cluster of hydrophobic side chains. Remarkably, A and B chains make unequal contributions to this folded moiety; the B chain retains nativelike supersecondary structure, whereas the A chain is largely disordered. These observations suggest that the B subdomain provides a template to guide folding of the A chain. Stepwise organization of insulin-like molecules supports a hierarchic view of protein folding.

Insulin is a globular protein containing two chains, designated A (21 residues) and B (30 residues) (*1*). Stored as a Zn^{2+}-stabilized hexamer in the human β cell, the hormone functions as a Zn^{2+}-free monomer (*2*). Despite its small size, insulin contains representative features of larger proteins, including canonical elements of secondary structure and a well-ordered hydrophobic core (*3*). The protein contains three disulfide bridges, two between chains (cystines A7−B7 and A20−B19) and one within the A chain (cystine A6−A11). Oxidative refolding of proinsulin and insulin chain combination in each case lead to native disulfide pairing (*4*−*7*). Studies of proinsulin-like molecules by air oxidation or redox-coupled disulfide exchange have revealed a preferred pathway of populated intermediates (Figure 1A; *8*−*15*). The study presented here focuses on the role of the A7−B7 disulfide bridge in protein folding and stability. Unlike internal cystines A20−B19 and A6−A11, the A7−B7 disulfide bridge lies on the protein surface[1] (Figure 1B). Although previous studies of an active analogue with a noncleavable aliphatic bridge between residues A7 and B7 suggested that the sulfur atoms are not required per se for receptor recognition[2] (*16*), it is not known whether cystine A7−B7 contributes to the hormone's receptor-binding surface. We describe herein pairwise substitution of Cys^{A7} and Cys^{B7} with serine in an engineered insulin monomer (DKP-insulin).[3] The analogue (designated DKP-*des*-[A7−B7]^{Ser}) provides a model of a late folding intermediate (*15*, *17*). Dramatic decreases in the analogue's stability and

† This work was supported by grants from the extramural diabetes program of National Institutes of Health to M.A.W. and P.G.K. and by the Diabetes Research and Training Center of The University of Chicago (S.H.N. and M.A.W.).

* To whom correspondence should be addressed. M.A.W.: e-mail, weiss@biochemistry.cwru.edu; telephone, (216) 368-5991; fax, (216) 368-3419. P.G.K.: e-mail, Panayotis.Katsoyannis@mssm.edu; telephone, (212) 241-9350; fax, (212) 996-7214.

‡ Case Western Reserve University School of Medicine.

§ The University of Chicago.

|| Mount Sinai School of Medicine of New York University.

[1] Abbreviations: BPTI, bovine pancreatic trypsin inhibitor; DKP-insulin, monomeric insulin analogue containing three substitutions in the B chain (Asp^{B10}, Lys^{B28}, and Pro^{B29}; see Table 1); DKP-*des*-[A7−B7]^{Ser}, insulin analogue containing substitutions Ser^{A7} and Ser^{B7} as well as DKP substitutions in the B chain (See Table 1); DQF-COSY, double-quantum-filtered correlation spectroscopy; IGF-I, insulin-like growth factor I; NMR, nuclear magnetic resonance; NOE, nuclear Overhauser enhancement; NOESY, NOE spectroscopy; HPLC, high-performance liquid chromatography; SA, simulated annealing; TOCSY, total correlated spectroscopy; 2D NMR, two-dimensional NMR.

[2] Cystine A7−B7 lies on the surface of the T-state protomer (*3*), which is the predominant conformation of insulin as a monomer in solution (*34*, *39*, *79*). However, following the T → R transition (an allosteric feature of insulin hexamers; *63*, *65*), cystine A7−B7 lies within a hydrophobic cleft between the A and B chains (see Figure 8); its torsion angle also undergoes a change in handedness (*64*).

[3] Studies of [A7,B7-L,L-2,7-diaminosuberoyl]-*des*-(B26−B30)-insulin B25-amide (an analogue in which the A7−B7 disulfide bridge was replaced with an aliphatic linker) by Brandenburg and colleagues (*16*) suggest that the sulfur atoms are not specifically required for activity but do not address whether the polarity of the tether influences biological activity. The analogue was only partially purified, however, precluding rigorous assessment of its biological activity. Previous studies of analogues containing A7 and B7 modifications (*80*−*82*) were performed prior to HPLC purification of monocomponent insulins. Although activities in the range of 0.3−15% were reported, the possibility of contamination by native insulin cannot be excluded.

10.1021/bi011021o CCC: $20.00 © 2001 American Chemical Society
Published on Web 09/15/2001

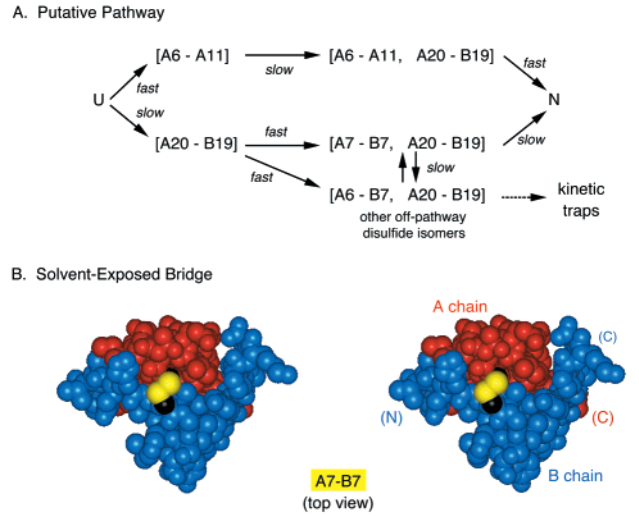

FIGURE 1: Putative disulfide pathway of proinsulin and role of the A7−B7 disulfide bridge. (A) Proposed pathway based on biochemical mapping studies of proinsulin-like molecules (*15*). U designates the unfolded and reduced polypeptide; N designates the native state with three disulfide bridges (A6−A11, A7−B7, and A20−B19). Intermediate species are designated by cystine(s); e.g., [A20−B19] indicates a species containing one disulfide bridge. The designations "fast" or "slow" refer to the recent kinetic study of Feng and co-workers (*15*). Technical limitations in peptide mapping precluded unambiguous assignment of disulfide pairing schemes, so the proposed pathway is in part hypothetical. (B) van der Waals surface representation of porcine insulin showing solvent-accessible positions of cystine A7−B7. The two sulfur atoms are shown in yellow and C_β methylene groups in black. The A chain is otherwise shown in red and the B chain in blue. The orientation is a "top view" relative to the standard depiction of insulin (see Supporting Information). The position of cystine A7−B7 in relation to insulin's putative receptor-binding surface is shown in Figure 8. Coordinates were obtained from the crystal structure of a T_6 insulin hexamer [molecule 1 (Chinese nomenclature) of 2-Zn insulin (*3*), and PDB entry 4INS].

function illuminate the essential role of the A7−B7 cross-link in stabilizing insulin's structure and function.[4]

Insulin is generated in vivo by proteolytic processing of a single-chain precursor, designated proinsulin, in which a connecting peptide joins the C-terminus of the B chain to the N-terminus of the A chain (*18*). Proinsulin and a variety of related single-chain analogues are employed in recombinant methods of pharmaceutical manufacture (*6*, *19*−*21*). That the connecting peptide acts only as a passive topological tether (i.e., it enables disulfide pairing to occur as an intramolecular process but is otherwise without specific folding information) has been demonstrated by two complementary lines of evidence. First, "reverse proinsulin", a topological analogue in which a rearranged connecting peptide links the N-terminus of the B chain to the C-terminus of the A chain, exhibits folding properties similar to those of native proinsulin (*22*). Second, under suitable conditions, air oxidation of isolated A and B chains preferentially yields covalent A−B heterodimers with native disulfide pairing (*4*). This reaction is known as *insulin chain combination.* The absence of detectable disulfide isomers indicates that folding information intrinsic to proinsulin's sequence resides within isolated A and B chains (*7*). Sequence specificity is highlighted by the exquisite sensitivity of chain combination yield to a subset of mutations in either chain (*23*). The extent to which this reaction is under thermodynamic versus kinetic control is not well understood.

Table 1: Design of Insulin Analogues[a]

	substitution	location	purpose
B10	His → Asp	surface of α-helix	destabilize trimer
B28	Pro → Lys	surface of β-strand	destabilize dimer
B29	Lys → Pro	surface of β-strand	destabilize dimer
A7	Cys → Ser	exposed disulfide bridge	untether A and B chains
B7	Cys → Ser	exposed disulfide bridge	untether A and B chains

[a] DKP-insulin contains three B chain substitutions, whereas DKP-*des*-[A7−B7]^{Ser} contains five substitutions; the latter retains native A6−A11 and A20−B19 disulfide bridges. The B28−B29 inversion was motivated by homology to IGF-I to destabilize insulin's classical dimer interface (*32*). Asp^{B10} destabilizes the hexamer interface (*33*).

Similarities between folding of proinsulin and insulin chain combination suggest that analogous mechanisms in each case specify the fidelity of disulfide pairing. Accordingly, insulin analogues lacking one or more disulfide bridges may be regarded as peptide models of protein-folding intermediates (*24*). Design of such analogues is based on biochemical characterization of the disulfide pathway of a single-chain insulin precursor (Figure 1A; *15*). As previously observed in studies of insulin-like growth factor I (IGF-I) (*8*−*10*, *13*, *17*), oxidative refolding of the precursor polypeptide proceeds through a discrete and nonrandom set of populated disulfide species, which presumably represent both on- and off-pathway intermediates (*25*). The productive pathway is not unique as at least two interconnected channels lead to the native state (Figure 1A). In one channel, the final disulfide bridge (cystine A7−B7) lies on the protein surface, whereas in the other, it is internal (A6−A11). Terminal formation of an exposed disulfide bridge is a hallmark of the oxidative pathway of the bovine pancreatic trypsin inhibitor (BPTI) (*26*, *27*). The native-like structure of the preceding two-disulfide BPTI intermediate orients the terminal thiolates for rapid oxidation. The celebrated complexities of the BPTI disulfide pathway arise in part due to kinetic barriers to further oxidation of native-like intermediates (*26*). Because BPTI analogues containing a single disulfide bridge exhibit native-like structure (*28*−*30*), the process of subsequent disulfide pairing and rearrangement may be unrelated to general mechanisms of hierarchical folding in a funnel-like landscape.

We demonstrate here that formation of a terminal solvent-exposed disulfide bridge in a protein may be accompanied by substantial local and nonlocal protein folding. Design of the present two-disulfide insulin analogue utilizes an engineered monomer (DKP-insulin; *31*−*33*) as a template to avoid confounding effects of self-association. The analogue thus contains additional substitutions in the B chain that weaken the hormone's classical dimer- and hexamer-forming surfaces (His^{B10} → Asp, Pro^{B28} → Lys, and Lys^{B29} → Pro; Table 1). The parent analogue retains a native T-state structure in solution (*32*, *33*) and exhibits twice the biological activity of native human insulin (*34*). Pairwise substitution of Cys^{A7} and Cys^{B7} with serine is shown to lead to substantial protein unfolding with a profound decrease in global

[4] While this paper was in preparation, related analogue [Ser^{A7}, Ser^{B7}]-*des*-Thr^{B30}-insulin was obtained in low yield by biosynthetic expression of an insulin precursor (*59*). Consistent with the results presented in this paper, the two-disulfide analogue exhibits marked decreases in helix content (as probed by CD) and function as evaluated in vivo using a rat hypoglycemic convulsion assay.

thermodynamic stability. Remarkably, ^{1}H NMR studies demonstrate that the A and B chains make asymmetric contributions to the folded moiety. Whereas the A chain is largely disordered, the B chain retains native-like supersecondary structure. Unlike the corresponding analogue of IGF-I (*35*), DKP-*des*-[A7−B7] exhibits extremely low activity. The A7−B7 disulfide bridge thus stabilizes key determinants of insulin's biological activity and may itself engage the insulin receptor. The novel partial fold of DKP-*des*-[A7−B7]^{Ser} provides strong support for a hierarchic model of proinsulin folding and insulin chain combination as a stepwise conformational search among a redox-sensitive series of energy landscapes.

EXPERIMENTAL PROCEDURES

Materials. 4-Methylbenzhydrylamine resin (0.63 mmol of amine/g; Bachem, Inc.) was used as solid support for synthesis of the A chain analogue; *N*-butoxycarbonyl-*O*-benzylthreonine-PAM resin (0.6 mmol/g; Bachem, Inc.) was used as solid support for synthesis of the B chain analogue. *tert*-Butoxycarbonyl amino acids and derivatives were obtained from Bachem, Inc. Amino acid analyses of synthetic chains and insulin analogues were performed after acid hydrolysis with a Hewlet Packard Amino Quant Analyzer (model 1090). Chromatography resins CM52 and DE52 cellulose (Whatman) and Cellex E (Ecteola cellulose; Sigma) were used.

Peptide Synthesis. The protocol for solid-phase synthesis is as described previously (*36*). The C-terminal Asn in synthesis of the A chain was incorporated into a solid support by coupling *tert*-butoxycarbonylaspartic acid α-benzyl ester with 4-methylbenzhydrylamine resin. After the final deprotection, the Asp residue was converted to an Asn residue.

(i) Synthesis of A Chain S-Sulfonate. From 3 g of 4-methylbenzhydrylamine resin, 8 g of peptidyl A chain resin was obtained. Peptidyl resin (0.7 g), after deblocking and sulfitolysis, yielded 220 mg of crude A chain, which on chromatography on a Cellex E column (*23*, *34*) afforded 88 mg of purified S-sufonated (A7^{Ser}) chain. Amino acid analysis gave the following ratios, in agreement with the theoretically expected values shown in parentheses: $Asp_{2.0\ (2)}$, $Thr_{1.0\ (1)}$, $Ser_{2.7\ (3)}$, $Glu_{4.2\ (4)}$, $Gly_{1.0\ (1)}$, $Val_{0.9\ (1)}$, $Ile_{1.8\ (2)}$, $Leu_{2.1\ (2)}$, and $Tyr_{2.1\ (2)}$; the level of Cys was not determined.

(ii) Synthesis of B Chain S-Sulfonate. From 1.3 g of *N*-butoxycarbonyl-*O*-benzylthreonine-PAM resin, 5.1 g of peptidyl B chain resin was obtained. Peptidyl resin (0.8 g), after deblocking and sulfitolysis, yielded 474 mg of crude B chain, which on chromatography on a DE52 cellulose column (*23*, *34*) afforded 133 mg of purified S-sulfonated DKP [Ser^{B7}] chain. Amino acid analyses gave the following ratios, in agreement with expected values: $Asp_{2.0\ (2)}$, $Thr_{1.7\ (2)}$, $Ser_{1.8\ (2)}$, $Glu_{3.0\ (3)}$, $Gly_{2.9\ (3)}$, $Ala_{1.0\ (1)}$, $Val_{3.1\ (3)}$, $Leu_{4.1\ (4)}$, $Tyr_{2.0\ (2)}$, $Phe_{2.9\ (3)}$, $His_{0.9\ (1)}$, $Lys_{0.9\ (1)}$, and $Arg_{1.0\ (1)}$; the levels of Pro and Cys were not determined.

Interaction of Derivatives. Chain combination was effected by interaction of the S-sulfonated derivatives of [A7^{Ser}] A chain (40 mg) and DKP [B7^{Ser}] B chain (20 mg) in 0.1 M glycine buffer (pH 10.6, 10 mL) in the presence of dithiothreitol (5.0 mg). Purification of the combination mixture by CM52 cellulose chromatography led to the isolation of 2.1 mg of the hydrochloride of the analogue as described previously (*23*, *34*). Final purification of this product by reversed-phase high-performance liquid chromatography (HPLC) yielded 0.3 mg of the purified insulin analogue. Amino acid ratios were as follows: $Asp_{3.8\ (4)}$, $Thr_{2.6\ (3)}$, $Ser_{4.7\ (5)}$, $Glu_{6.7\ (7)}$, $Gly_{4.2\ (4)}$, $Ala_{1.1\ (1)}$, $Val_{3.8\ (4)}$, $Ile_{1.5\ (2)}$, $Leu_{6.1\ (6)}$, $Tyr_{3.6\ (4)}$, $Phe_{3.0\ (3)}$, $His_{0.9\ (1)}$, $Lys_{0.9\ (1)}$, and $Arg_{0.9\ (1)}$; the levels of Pro and Cys were not determined. The analogue's predicted molecular mass (5755.8 Da) was verified (5757.3 Da) by electrospray mass spectrometry.

Peptide Mapping of DKP-des-[A7−B7]^{Ser}. Digestion of DKP-insulin and DKP-*des*-[A7−B7]^{Ser} analogues by *Staphylococcus aureus* V8 protease (Pierce) enabled mapping of disulfide-containing peptide fragments (*6*). The reaction was carried out with 10 and 2 μg of analogue and enzyme, respectively, in 0.16 mL of 0.05 M Tris-HCl (pH 8.0) at 37 °C for 5 h. A portion (40 μL) of the digested mixture was acidified by the addition of neat acetic acid (10 μL), and the sample (40 μL) was analyzed by reverse-phase HPLC on a Microsorb C18 column (0.46 cm × 25 cm, Rainin) using an elution gradient between an aqueous mixture of 0.1 M phosphoric acid and 0.02 M triethylamine (adjusted to pH 3.0 with NaOH) and acetonitrile. The concentration of acetonitrile was 15% (v/v) at the start and was increased at a rate of 1%/min. Absorbance was measured at 214 nm using a Perkin-Elmer series 4 chromatographic system and an LC-85 UV detector. In the chromatogram corresponding to DKP-insulin, three peaks were observed corresponding to peptides containing residues (i) B22−B30, (ii) A18−A21 in disulfide linkage to B14−B21, and (iii) A5−A17 in disulfide linkage to B1−B10. In the chromatogram corresponding to DKP-*des*-[A7−B7]^{Ser}, peak iii did not exist. Instead, two new peaks were observed, corresponding to the A5−A17 and B1−B10 fragments due to a lack of an A7−B7 disulfide linkage.

Biological Assays. Receptor binding studies were performed using a human placental membrane preparation as described previously (*37*). Relative activity is defined as the ratio of analogue to human insulin required to displace 50% of specifically bound ^{125}I-labeled human insulin (purchased from Dupont Amersham).

Spectroscopy. ^{1}H NMR spectra were obtained at 600 MHz and 25 °C in 50 mM potassium phosphate (pH 7.0) and independently in 20% deuterioacetic acid (pH 1.9) as described previously (*34*, *38*); the protein concentration was 1.5 mM. Spectra in H_2O were obtained using pulse-field gradients and laminar-shaped pulses (*34*). CD spectra were obtained using an Aviv spectropolarimeter equipped with thermister temperature control and an automated titration unit for guanidine denaturation studies. CD samples for wavelength spectra contained 25−50 μM insulin analogue in 50 mM potassium phosphate (pH 7); samples were diluted to 5 μM for equilibrium denaturation studies.

NMR Resonance Assignment. The NMR spectrum of DKP-*des*-[A7−B7]^{Ser} at neutral pH was partially interpreted by a bootstrap strategy; sequential assignment was obtained in 20% deuterioacetic acid (*38*) and extended by analogy to neutral pH (*34*). This approach exploits a fortuitous narrowing of shifted resonances in the organic cosolvent, presumably due to more complete averaging of chemical shifts on the NMR time scale. Sequential assignment in the cosolvent system was based on DQF-COSY, TOCSY (mixing time of 55 ms), and NOESY (mixing time of 200 ms) spectra. Associated $^3J_{\alpha N}$ coupling constants in the folded moiety could

Table 2: Properties of Insulin Analogues[a]

analogue	ΔG_u	$\Delta\Delta G_u$	C_{mid} (M)	m (kcal mol^{-1} M^{-1})	potency (%)
DKP-insulin	4.9 ± 0.1	−	5.8 ± 0.1	0.84 ± 0.01	161 ± 19
DKP-*des*-[A6−A11]^{Ala}	1.4 ± 0.4	−3.5 ± 0.5	2.7 ± 0.4	0.52 ± 0.08	5
DKP-*des*-[A6−A11]^{Ser}	1.9 ± 0.3	−3.0 ± 0.4	2.9 ± 0.3	0.65 ± 0.07	0.1
DKP-*des*-[A7−B7]^{Ser}					
fit 1	0.3 ± 0.6	−4.6 ± 0.7	0.7 ± 1.1	0.48 ± 0.05	0.002
fit 2	0.5 ± 0.1	−4.4 ± 0.2	1.2 ± 0.3	0.46 ± 0.03	
fit 3	0.3 ± 0.2	−4.6 ± 0.3	0.9 ± 0.3	0.34 ± 0.02	

[a] ΔG_u indicates the apparent change in free energy on denaturation in guanidine-HCl as extrapolated to zero denaturant concentration by a two-state model. $\Delta\Delta G_u$ indicates the difference in ΔG_u values relative to that of DKP-insulin. Thermodynamic differences between DKP-*des*-[A6−A11]^{Ala} and DKP-*des*-[A6−A11]^{Ser} are not significant. Uncertainties in two-state fitting parameters do not include possible systematic error due to non-two-state behavior. C_{mid} is defined as that concentration of guanidine-HCl at which 50% of the protein is unfolded. The m value provides the slope in plotting the unfolding free energy ΔG_u ([G_u·HCl]) vs the molar concentration of denaturant; this slope is proportional to the protein surface area exposed on unfolding. Potencies are expressed as percent affinity for the human placental insulin receptor, defined relative to native human insulin (100%). Fits 1−3 in the analysis of DKP-*des*-[A7−B7]^{Ser} designate nonlinear least-squares fitting assuming (1) simultaneous fitting of slopes of pre- and post-transition baselines, (2) a horizontal pretransition baseline with simultaneous fitting of the slope of the post-transition baseline only, or (3) horizontal pre- and post-transition baselines without fitting of either slope (see Experimental Procedures).

not be inferred from DQF-COSY $H_\alpha-H_N$ cross-peaks as conformational broadening leads to antiphase cancellation. The bootstrap procedure is justified by insulin's native structure in 20% deuterioacetic acid (*34*, *39*), overall similarities between the analogue's spectra under the two conditions, and the consistency between NMR-derived helix content in the cosolvent system and CD-derived helix content at neutral pH (see the Results). Tables of chemical shifts and additional NMR spectra are provided as Supporting Information.

Thermodynamic Modeling. Guanidine denaturation data were fitted by a nonlinear least-squares method to a two-state model as described previously (*40*). In brief, CD data $\theta(x)$, where x indicates the concentration of denaturant, were fitted by a nonlinear least-squares program according to

$$\theta(x) = \frac{\theta_A + \theta_B e^{(-\Delta G^\circ_{H2O} - mx)/RT}}{1 + e^{(-\Delta G^\circ_{H2O} - mx)/RT}}$$

where x is the concentration of guanidine and where θ_A and θ_B are baseline values in the native and unfolded states, respectively. These baselines were approximated by pre- and post-transition lines $\theta_A(x) = \theta_A{}^{H_2O} + m_A x$ and $\theta_B(x) = \theta_B{}^{H_2O} + m_B x$. Fitting the original CD data and baselines simultaneously circumvents artifacts associated with linear plots of ΔG as a function of denaturant according to $\Delta G^\circ(x) = \Delta G^\circ_{H_2O} + m^\circ x$ (for reviews, see refs *40* and *41*). Because the nonsigmoidal shape of the unfolding transition makes definition of pre- and post-transition baselines uncertain, modeling was also performed assuming that (i) $\theta_A(x) = \theta_A{}^{H_2O}$ with fitting of only the post-transition baseline and (ii) $\theta_A(x) = \theta_A{}^{H_2O}$ and $\theta_B(x) = \theta_B{}^{H_2O}$ without either baseline fitting (see Table 2). The consistency of extracted parameters indicates that results are robust to baseline uncertainties within the limits of the two-state model. The m values obtained in fitting the variant unfolding curve are in each case significantly lower than the m value obtained in fitting the wild-type unfolding curve (DKP-insulin; see Table 2). This situation can be associated with an underestimate of the analogue's stability. The analogue's lower m value may reflect its more exposed hydrophobic surface in the absence of denaturant and/or existence of a native-state ensemble containing a distribution of incompletely folded forms of differing stability (*41*). Analysis of unfolding curves in this setting has recently been considered by Luo and Baldwin in a study of an equilibrium molten globule (apomyoglobin; *42*). In this formalism, an upper bound to the stability of the analogue is obtained by multiplying its $\langle C_{mid} \rangle$ value (an apparent value reflecting an average over an ensemble of distinct partial folds) by the native m value.

RESULTS

DKP-*des*-[A7−B7]^{Ser} was prepared by total synthesis (see Experimental Procedures). The analogue contains one substitution in the A chain and four in the B chain (Table 1). Protein design is based on DKP-insulin, a high-activity engineered monomer (*32*, *33*). The yield of DKP-*des*-[A7−B7]^{Ser} on chain combination was 3-fold lower than that observed in the synthesis of DKP-insulin.[5] The presence of native A6−A11 and A20−B19 disulfide pairings in the HPLC-purified DKP-*des*-[A7−B7]^{Ser} product was verified by peptide mapping. The biological activity of DKP-*des*-[A7−B7]^{Ser}, measured by analysis of specific binding to the insulin receptor, was found to be 0.002% ($K_d = 4.5 \times 10^{-5}$ M) relative to the activity of human insulin. This represents an extraordinary reduction of 10^5-fold relative to that of DKP-insulin (*20*, *33*); mutations in the putative receptor-binding surface ordinarily exhibit decreases in affinity of less than 10^3-fold (and usually less than 10^2-fold; *3*). The corresponding analogue of IGF-I (Ser6, Ser48) retains 0.3% native affinity for the type I IGF-I receptor[6] (*12*, *35*).

Analogue Exhibiting a Novel Partial Fold. The far-ultraviolet (UV) circular dichroic (CD) spectrum of DKP-*des*-[A7−B7]^{Ser} at 4 °C provides evidence of a partial fold. The analogue exhibits decreased helix content [asterisk in Figure 2A (○)] relative to the parent DKP-insulin monomer (●). The extent of attenuation is more marked than that previously observed in studies of DKP-*des*-[A6−A11]^{Ser} (Figure 2B). To evaluate the thermodynamics of protein unfolding, denaturation in guanidine-HCl was monitored at a helix-sensitive wavelength of 222 nm (Figure 2C). DKP-insulin exhibits a cooperative unfolding transition with a two-state free energy (ΔG_u) of 4.9 ± 0.1 kcal/mol (line 1 in Table 2; *43*) as estimated by nonlinear least-squares fitting. Pairwise

[5] In contrast to the results presented here, synthetic studies of DKP-*des*-[A6−A11]^{Ser} and DKP-*des*-[A6−A11]^{Ala} demonstrated chain combination yields similar to that of DKP-insulin (*34*, *43*). A related analogue was also investigated by others (*83*).

[6] Analysis of the IGF-I analogue's structure and stability by CD, guanidine titration, and fluorescence (*35*) suggests perturbations similar to those described here. Although the extent of ^{1}H NMR chemical shift dispersion was likewise reduced, NOESY spectra demonstrated retention of a native-like I43−Y60 contact, corresponding to packing of Ile^{A2} and Tyr^{A19} in insulin. The latter NOE is not observed in DKP-*des*-[A7−B7]^{Ser}, suggesting a less compact structural ensemble.

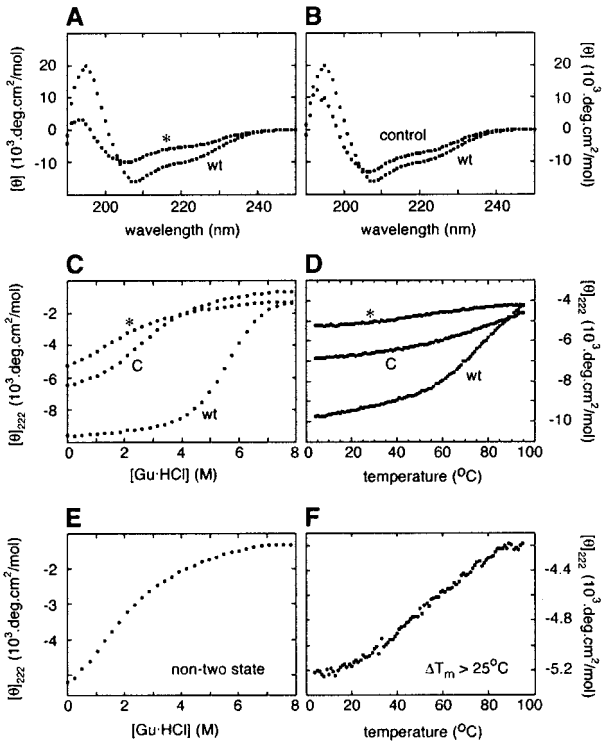

FIGURE 2: CD studies of an insulin analogue demonstrating the marked loss of structure and thermodynamic perturbation. (A and B) Untethering of cystine A7−B7 leads to more severe loss of structure than does untethering of cystine A6−A11: (A) far-UV CD spectrum of DKP-*des*-[A7−B7]^{Ser} (asterisk) relative to the spectrum of DKP-insulin (wt) and (B) CD spectrum of DKP-*des*-[A6−A11]^{Ser} (control) relative to the spectrum of DKP-insulin (wt). (C and D) Guanidine unfolding curves (C) and thermal unfolding curves (D) of *des*-[A7−B7]^{Ser} (asterisk) relative to those of DKP-*des*-[A6−A11]^{Ser} (C) and DKP-insulin (wt). (E) Expansion of the guanidine unfolding curve of DKP-*des*-[A7−B7]^{Ser} highlights the nonsigmoidal character of the transition. (F) Expansion of the thermal curve of DKP-*des*-[A7−B7]^{Ser} highlights the extent of destabilization (T_m > 25 °C). Thermodynamic parameters derived from guanidine titration curves are given in Table 2.

substitution of cystine A6−A11 with either alanine or serine leads to a similar destabilization (estimated change in free energy $\Delta\Delta G_u$ of 3 ± 0.3 kcal/mol; lines 2 and 3 in Table 2) with retention of sigmoidal cooperativity. Inspection of unfolding curves suggests that DKP-*des*-[A7−B7]^{Ser} is even less stable. Further, the shape of the curve exhibits a qualitative change: lack of sigmoidal character (see the asterisk in Figure 2C and expansion in Figure 2E), suggesting possible non-two-state unfolding. Although application of the two-state formalism is complicated by unclear pre- and post-transition baselines, experimental points are consistent with a two-state function of the form

$$\theta(x) = \frac{\theta_A + \theta_B e^{(-\Delta G^\circ_{H2O} - mx)/RT}}{1 + e^{(-\Delta G^\circ_{H2O} - mx)/RT}}$$

as fit by a nonlinear least-squares algorithm (*40*). Three modeling procedures each yield χ^2 values greater than 0.999: simultaneous fitting of ΔG_u, *m*, and pre- and post-transition baselines (fit 1 in Table 2), simultaneous fitting of ΔG_u, *me*, and the post-transition baseline (fit 2 in Table 2), and fitting of ΔG_u and *m* with fixed horizontal pre- and post-transition baselines (fit 3 in Table 2). The models each

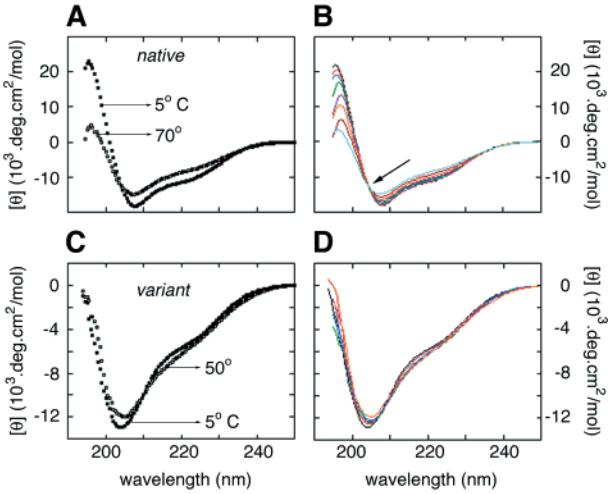

FIGURE 3: Non-two-state thermal unfolding of a two-disulfide analogue. (A and B) Control studies of DKP-insulin. (A) Far-UV CD spectra of DKP-insulin at 5 and 70 °C indicate partial loss of helix content. (B) Comparison of multiple spectra at 5 (black), 10 (red), 20 (blue), 30 (green), 40 (fushia), 50 (yellow), 60 (brown) and 70 °C (light blue) indicates the presence of an isoasbestic point (arrow) consistent with a two-state unfolding transition. (C and D) Parallel CD studies of DKP-*des*-[A7−B7]^{Ser} reveal the less marked effects of temperature and the absence of an isoasbestic point.

predict an apparent value for ΔG_u of <1 kcal/mol and hence value for $\Delta\Delta G_u$ of >3.9 kcal/mol.

The models also imply a significant reduction in the *m* value (column 5 in Table 2; *44*), consistent with a change in the extent of hydrophic exposure of DKP-*des*-[A7−B7]^{Ser} that is smaller than that which occurs on denaturation of DKP-insulin or DKP-*des*-[A6−A11]^{Ser}. This is as expected given that under native conditions DKP-*des*-[A7−B7]^{Ser} is already substantially unfolded. In the setting of a reduced *m* value, however, it is possible that the fitted value of ΔG_u underestimates the actual ΔG_u (*41*). An upper bound may be estimated by the formalism of Luo and Baldwin, developed to measure the average stability in a heterogeneous system, such as a distribution of incompletely folded forms (*42*). The apparent C_{mid} is regarded as the ensemble average of $C_{mid,i}$ values due to species *i* with fractional contribution α_i:

$$\langle C_m \rangle = \sum \alpha_i C_{mi}$$

An upper bound for the stability of the heterogeneous system is obtained as the product of $\langle C_{mid} \rangle$ and the native *m* value. Use of the maximal C_{mid} value obtained by two-state modeling (1.8 M; upper bound of 0.7 ± 1.1 M; see fit 1 in Table 2) yields 1.5 kcal/mol as an upper bound for ΔG_u. The profound instability of DKP-*des*-[A7−B7]^{Ser} is thus robust to choice of model.

Analogous instability is seen in thermal unfolding. DKP-*des*-[A7−B7]^{Ser} exhibits incremental and progressive attenuation of ellipticity with increasing temperature. The apparent thermal unfolding midpoint (T_m) is reduced by at least 25 °C relative to that of DKP-insulin. Because the two-disulfide analogue exhibits an attenuated helix content under native conditions, the decrease in helix content observed at high temperature is smaller than that seen in control studies of DKP-insulin (Figure 3A,C). Non-two-state behavior in thermal unfolding is suggested by the absence of an isoasbestic point in a series of CD spectra obtained at

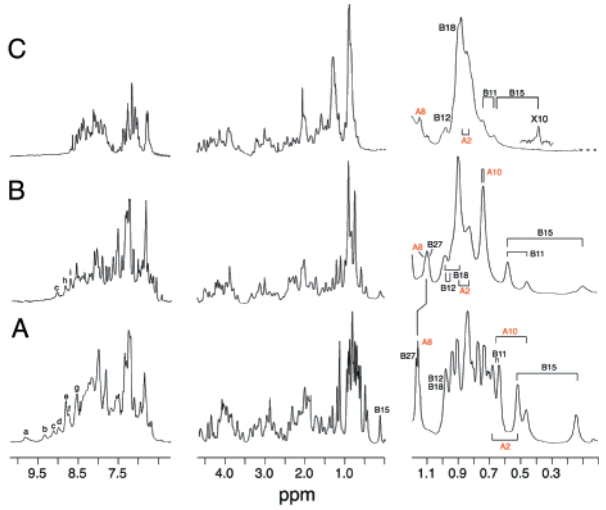

FIGURE 4: ^{1}H NMR spectrum of DKP-*des*-[A7−B7]^{Ser} at neutral pH in aqueous solution exhibiting a loss of dispersion: (A) DKP-insulin, (B) DKP-*des*-[A6−A11]^{Ser}, and (C) DKP-*des*-[A7−B7]^{Ser}. The relative changes in chemical shift dispersion are in accord with relative helix contents as inferred from CD (see Figure 2). Selected assignments of aliphatic resonances, including the upfield spin system of Leu^{B15}, are as labeled. Amide assignments in spectrum A are as described (*41*): A11, B8, B9, B6, B7, B19, B5, B7, and B19. Corresponding spectra in 20% deuterioacetic acid (Supporting Information) exhibit similar features. The amino acid substitutions in DKP-insulin and DKP-*des*-[A7−B7]^{Ser} are given in Figure 5 and Table 1.

successive temperatures (Figure 3D). DKP-insulin by contrast exhibits a classical isoasbestic point (arrow in Figure 3B).

Asymmetric Unfolding of the A and B Chains. The ^{1}H NMR spectrum of DKP-*des*-[A7−B7]^{Ser} (pH 7.2 and 25 °C) exhibits a reduction in dispersion relative to the spectrum of DKP-*des*-[A6−A11]^{Ser}, which itself exhibits less dispersion than that of DKP-insulin (Figure 4). Analysis of two-dimensional (2D) ^{1}H NMR spectra under these conditions is limited by a combination of poor resolution (for those resonances with near-random coil chemical shifts) and differential line broadening (for those resonances with significant secondary chemical shifts). Because the extent of broadening is not significantly affected by protein concentration in the range of 0.2−1.5 mM and occurs in the context of sharp resonances elsewhere in the spectum, such broadening is ascribed to conformational exchange on the (millisecond) time scale of NMR chemical shifts; some additional broadening due to transient self-association cannot be excluded. The combination of narrow and broad resonances suggests that the analogue contains a molten subdomain flanked by disordered segments. Sequential assignment in 20% deuterioacetic acid (Figure 5A; see also Supporting Information) demonstrates retention of a native-like B9−B19 α-helix and A16−A19 partial helical segment. Observation of protected amide resonances in a D_2O solution [Figure 5A (○)] indicates that peptide hydrogen bonds are stably maintained in the folded moiety. Native helical segments of residues A2−A8 and A12−A15 are not observed. Loss of α-helix in the A chain is consistent with the decreased overall helix content of DKP-*des*-[A6−A11]^{Ala} as inferred by CD. Two main chain d_{NN} NOEs are seen within the A6−A11 segment, presumably due to nonrandom conformational preferences near cystine A6−A11.

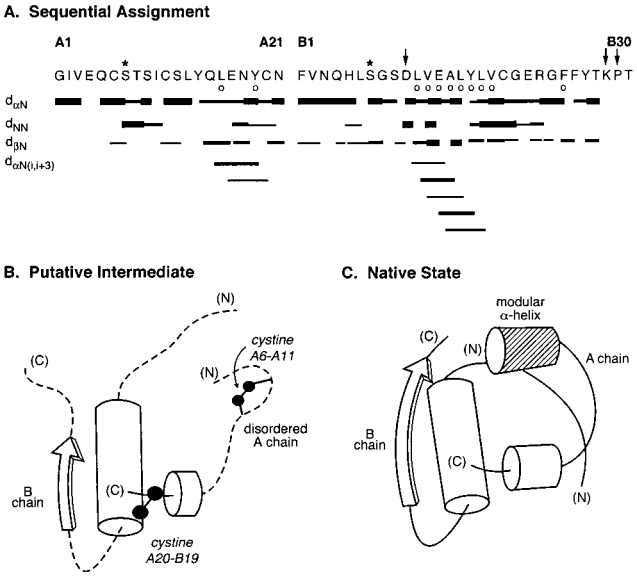

FIGURE 5: ^{1}H NMR signature of α-helix and structural models. (A) Summary of the sequential resonance assignment of DKP-*des*-[A7−B7]^{Ser} in 20% deuterioacetic acid in Wüthrich format providing evidence of the A16−A19 helical turn and native-like B9−B19 helix. The A chain is shown by convention on the left and the B chain on the right (opposite to the order of corresponding sequences in the gene). Asterisks indicate sites of Cys → Ser substitutions; arrows indicate the three DKP substitutions in the B chain that yield a monomeric template (*33*). The intensity of the cross-peaks is represented in schematic fashion by the thickness of the line. Open circles indicate sites of slowly exchanging amide resonances in D_2O solution. (B and C) Cylinder models of DKP-*des*-[A7−B7]^{Ser} (B) and DKP-insulin (C). Dashed lines in model B denote disordered regions. The positions of the two native cystines in DKP-*des*-[A7−B7]^{Ser} are indicated by black bars and circles. The shaded helix in the native state (C) highlights the modularity of the N-terminal A-chain α-helix, whose segmental unfolding in DKP-*des*-[A6−A11]$^{Ala/Ser}$ is independent of the remainder of the protein (*43*).

Sequential assignment in the organic cosolvent system enables assessment of trends in chemical shifts (*38*). Whereas many resonances in the A chain exhibit near-random coil values, significant nonrandom shifts occur among the majority of B chain resonances. B chain secondary shifts in part recapitulate those of native insulin. An overview of such shifts (defined as differences between observed chemical shifts and tabulated random coil values) in DKP-*des*-[A7−B7]^{Ser} and DKP-insulin is provided in Figure 6; chain and region specific perturbations are coded by color. Almost all symbols are located in the lower-left triangle of each diagonal plot, reflecting the trend toward reduced chemical shift dispersion in the two-disulfide analogue. Symbols along the diagonal indicate resonances with similar secondary shifts in DKP-*des*-[A7−B7]^{Ser} and DKP-insulin; these predominantly occur in the B chain supersecondary structure and the A16−A20 segment. The distinctive upfield secondary chemical shifts of the methyl resonances of Leu^{B15}, for example, are retained with attenuated magnitude in both solvent systems. Tables of chemical shifts and chemical shift differences are provided as Supporting Information. A similar pattern of chemical shifts is observed at neutral pH and assigned by analogy.

Retention of long-range NOEs (between the side chains of Phe^{B24} and Leu^{B15} and between Tyr^{B26} and Val^{B12}) indicates that a native-like helix−turn−strand supersecondary

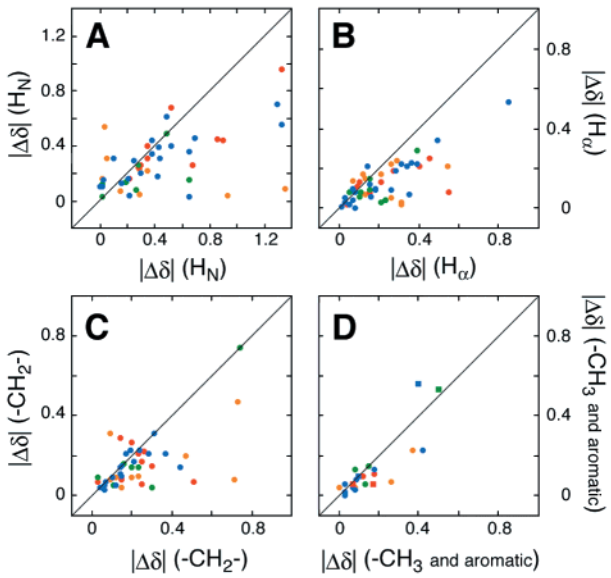

FIGURE 6: Asymmetric loss of chemical shift dispersion in the A and B chains. Magnitudes of secondary chemical shifts ($|\Delta\delta|$) are plotted by proton class; in each panel, the ordinate derives from DKP-insulin and the abscissa derives from DKP-*des*-[A7−B7]^{Ser}. The proton classes are as follows: (A) amide resonances, (B) Hα resonances, (C) methylene resonances, and (D) methyl and aromatic resonances. Assignments are color-coded by segment: (yellow) residues A1−A11, (orange) residues A12−A21, (green) residues B1−B8, and (blue) residues B9−B30. Partial unfolding of the two-disulfide analogue is manifest in each panel by points in the lower right-hand triangle. The preferential clustering of blue symbols along the diagonal line reflects chain-specific retention of B chain supersecondary structure in the B9−B26 segment.

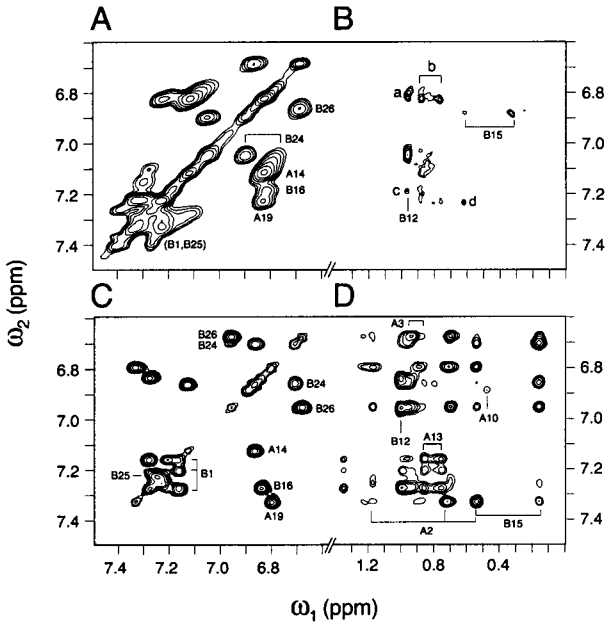

FIGURE 7: 2D 600 MHz ^{1}H NMR spectra of DKP-*des*-[A7−B7]^{Ser} at neutral pH in aqueous solution demonstrating an ordered moiety. (A) A TOCSY spectrum of aromatic spin systems reveals partial retention of chemical shift dispersion and line broadening. (B) The aligned portion of NOESY spectrum (mixing time of 200 ms) contains cross-peaks between aromatic side chains (vertical axis; ω_2) and aliphatic protons (horizontal axis; ω_1) in the folded moiety: Phe^{B24}−Leu^{B15} (indicated), (a) B16 Hε−B12 γCH$_3$, (b) A19 Hε−A16 δCH$_3$, (c) B16 Hδ−B12 γCH$_3$, and (d) A19 Hδ−B15 δCH$_3$. No contacts are observed between Tyr^{A19} and Ile^{A2}. (C and D) Corresponding TOCSY (C) and NOESY (D) spectra of DKP-insulin exhibit marked chemical shift dispersion and density of inter-residue contacts. Assignments are as shown. Spectra were obtained at 32 °C in D_2O (pD 7.6, direct meter reading).

structure is retained in the B chain.[7] As in DKP-insulin (*34*), a long-range NOE is observed between the side chains of Tyr^{A19} and Leu^{B15}, indicating a native-like hydrophobic cluster. Corresponding long-range NOEs are observed at neutral pH (Figure 7). No contacts are observed between Tyr^{A19} and Ile^{A2}, an otherwise invariant feature of insulin's native state (*3*). A schematic model of the folded moiety in DKP-*des*-[A7−B7]^{Ser} is shown in Figure 5B in relation to the native T state (Figure 5C). This model contains stable elements of secondary structure (cylinders) and disordered segments (dashed lines). Disorder is corroborated by motional narrowing of H_α−H_N resonances (A1−A5, B1−B6, and B27−B30), visualized in DQF-COSY spectra by robustness to antiphase cancellation (*45*) in the organic cosolvent. These residues exhibit no detectable nonlocal nuclear Overhauser effects (NOEs). The extent of organization in the proposed model is smaller than that observed in distance geometry models of DKP-*des*-[A6−A11]^{Ser} in which substantial structure was retained in the A chain and hydrophobic core (*43*).

DISCUSSION

Analogues of DKP-insulin lacking cystine A6−A11 (DKP-*des*-[A6−A11]^{Ser} and DKP-*des*-[A6−A11]^{Ala}) have previously been shown to exhibit segmental unfolding of the A1−A8 segment within an otherwise native-like fold (*34*, *43*). Here, we have extended this approach to investigate the consequences of untethering the solvent-exposed A7−B7 disulfide bridge. Our results demonstrate that DKP-*des*-[A7−B7]^{Ser} exhibits a more severe loss of ordered structure than was observed in studies of DKP-*des*-[A6−A11]^{Ser} or DKP-*des*-[A6−A11]^{Ala}. We outline in turn possible implications for structure−activity relationships and oxidative protein folding. Disulfide intermediates of insulin and related proteins exhibit stepwise structural organization with successive disulfide pairing (*12*, *35*, *46*). Similarities and differences between such hierarchical behavior and the oxidative refolding properties of model globular proteins (such as BPTI, α-lactalbumin, and ribonuclease A; *26*, *27*, *47*−*56*) are discussed.

Structure−Activity Relationships. Our previous study established that local unfolding of the internal A1−A8 α-helix in DKP-*des*-[A6−A11]^{Ala} (but not DKP-*des*-[A6−A11]^{Ser}) is compatible with significant biological activity (*43*). These results were consistent with an induced-fit model: the destabilized A1−A8 segment regains helical structure on receptor binding. The greater activity of the alanine analogue was rationalized on the basis of alanine's greater helical propensity (*43*, *57*) and hydrophobicity (*58*) relative to serine, local properties that would facilitate restoration of the A chain's native structure in the hormone−receptor complex.

[7] Observed long-range NOEs in partially folded species may in principle reflect either stably maintained or transient interactions, i.e., contacts present in only a subset of molecules at a given time in an ensemble of fluctuating structures. In contrast, maintenance of helix-related NOEs is corroborated by observation of slowly exchanging amide resonances in D_2O (see Figure 5A).

Untethering the exposed A7−B7 disulfide bridge leads to a 10^5-fold decrease in the level of receptor binding. A similarly profound loss of activity in vivo has recently been demonstrated using the rat convulsion assay (*59*). The present analogue's extraordinary decrease in the level of binding, greater in magnitude than the free energy of unfolding of DKP-insulin itself, may in part reflect destabilization of the hormone's receptor-binding surface (*3*, *60*−*62*) and in part a change in the environment of cystine A7−B7 on receptor binding. Two possible models are plausible, one based on the crystallographic T state and the other on the R state (*63*, *64*).

(i) Engagement of Cystine A7−B7 in the Hormone−Receptor Interface. The functional deficit of DKP-*des*-[A7−B7]^{Ser} raises the possibility that cystine A7−B7 directly engages the insulin receptor as previously suggested by Dodson and colleagues (*3*). In the structure of the crystallographic T state, the A7−B7 disulfide bridge protrudes from the surface (Figure 8A). Engagement of cystine A7−B7 at the interface would extend the known boundaries of insulin's receptor-binding surface (Figure 8A; *3*, *60*−*62*).

(ii) Packing of Cystine A7−B7 in the Nonpolar Crevice of the Hormone. The T → R transition, well characterized among crystallographic hexamers (*63*−*66*), is characterized by a change in the secondary structure of the B1−B8 segment from extended strand to α-helix. This transition is accompanied by changes in the dihedral angles of the A7−B7 disulfide bridge and Gly^{B8} (shown in black in Figure 8A). In the R state, cystine A7−B7 is largely buried in a hydrophobic cleft between chains (Figure 8B,C). Should aspects of the T → R transition be recapitulated on receptor binding, then the environment of the disulfide bridge could change from exposed and solvated (free hormone) to nonpolar and buried (bound hormone).

Either model could account for the very low activity of DKP-*des*-[A7−B7]$^{Ser'}$; in each case, cystine A7−B7 is proposed to pack within a nonpolar environment in the hormone−receptor complex. The polar *β*-OH groups of Ser^{A7} and/or Ser^{B7} would hence be expected to destabilize the variant complex, blocking induced fit. The general hypothesis that the environment of cystine A7−B7 changes from hydrophilic to hydrophobic on receptor binding can be tested by future characterization of an [Ala^{A7},Ala^{B7}] or related analogue containing nonpolar side chains at A7 and B7. Unfortunately, such experiments cannot distinguish between the models described above. Structural characterization of the local role of the A7−B7 disulfide bridge in receptor binding and assessment of the functional relevance of the T → R transition will require crystallographic analysis of a hormone−receptor complex.

It is surprising that corresponding serine substitutions in IGF-I cause only a 300-fold decrease in the level of binding to the type I IGF-I receptor[6] (*35*); the corresponding alanine analogue likewise exhibits a 100-fold decrement (*12*). Such a marked difference between insulin and IGF-I may indicate a difference in the mode of receptor binding. Differences are in principle possible in global positioning of the ligand with respect to the receptor or in the local environment of the cognate disulfide bridge in the ligand−receptor complex. Alternatively, it is possible that IGF-I, as a single-chain analogue, is less perturbed by loss of a long-range disulfide tether than is insulin as a two-chain molecule. Differences between homologous insulin− and IGF-I−receptor complexes have previously been demonstrated (*67*−*70*). It is not

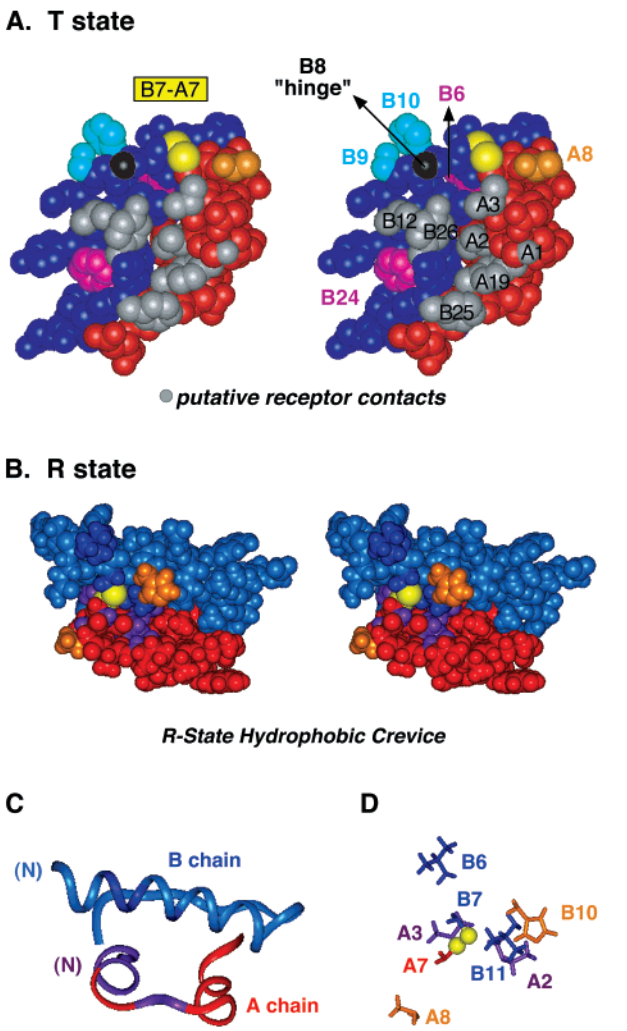

FIGURE 8: Putative receptor-binding surface of human insulin (gray) based on the crystallographic T and R states (*3*). (A) T-State model. Critical side chains of Ile^{A2}, Val^{A3}, and Tyr^{A19} are highlighted in the A chain along with the α-amino group of Gly^{A1}; critical side chains of Val^{B12}, Tyr^{B26}, and Phe^{B25} are highlighted in the B chain. Cystine A7−B7 (sulfur atoms shown as yellow balls) is exposed on the protein surface near these key determinants, most prominently Val^{A3}. The side chains of Ser^{B9} and His^{B10} (blue) are proposed to lie at one edge of the receptor interface, whereas Thr^{A8} (orange) is proposed to lie at the other. Side chains in gray indicate invariant surface sites at which mutations significantly impair activity; other portions of the A and B chains are shown in red and blue, respectively. Although this figure is based on the crystallographic T state, the active conformation of insulin is unknown. The side chain of Leu^{B11} is mostly buried in the T state (magenta) but might be exposed on a change in configuration of Gly^{B8} (C_α atoms shown in black). Another site of conformational change is suggested at Phe^{B24} (magenta) since, as a seeming paradox, its substitution with D-Phe or D-Ala enhances insulin's activity (*3*). Tyr^{B26} is not required for activity in the foreshortened analogue *des*-pentapeptide (B26-B30)-insulin amide. The extent of contact between insulin and its receptor is likely to be more extensive than the gray region shown. (B−D) R-State model. In a space-filling model (B), sulfur atoms of cystine A7−B7 (yellow) are predominantly buried in a crevice between the A and B chains. The orientation of chains is defined by a ribbon model (C). The hydrophobic character in this crevice is highlighted by color coding (aliphatic side chains of Leu^{B6}, Val^{A3}, Leu^{B11}, and Ile^{A2}; upper left to lower right in panels B and D).

known whether the conformational repertoire of IGF-I can include features of insulin's T → R transition and so whether model ii above is relevant to its mode of receptor binding.

Oxidative Protein Folding. Studies of model globular proteins have highlighted the principle that disulfide bridges reflect rather than direct protein structure. An illustration of this principle is provided by the demonstration of native structure in BPTI analogues lacking two of its three native disulfide bridges (*29*, *30*). The complex choreography of subsequent disulfide pairing and exchange in BPTI may thus be regarded as peripheral to the central problem posed by the conformational search of the unfolded-state ensemble[8] (*26*, *29*, *30*). Complementary insights have emerged from studies of ribonuclease A (*53*−*56*) and α-lactalbumin (*48*−*51*). An analogue of α-lactalbumin in which each of its eight cysteines has been substituted with alanine ("all-Ala-α-La") forms a compact molten structure with key native-like features (*52*). The various disulfide bridges play distinct roles in stabilizing the native state, however, depending in part on the intrinsic stability of neighboring long-range interactions. There would be little entropic penalty, for example, in forming a cross-link between segments of the polypeptide chain already in proximity in the reduced-state ensemble. We imagine that the hierarchical disulfide pathways of proinsulin and related proteins reflect analogous structural principles and propensities in this family of sequences. The associated hierarchy of partial folds nevertheless highlights a critical difference, the lower intrinsic stability of the native insulin fold.

The putative disulfide pathway of a single-chain insulin precursor (*15*) presumably begins with random disulfide pairing that rapidly reassorts to two predominant species, one containing cystine A20−B19 and the other containing cystine A6−A11. Although these two disulfide bridges are each buried in the native state, our results suggest a fundamental difference between their environments in populated intermediates. The A20−B19 disulfide bridge participates in and presumably stabilizes a molten subdomain, whereas the A6−A11 disulfide bridge spans a poorly ordered segment. We suggest that cystine A6−A11 is favored because of the proximity of these sites in the sequence and instability of alternative local pairing schemes (a vicinal A6−A11 disulfide bridge and A7−A11). In contrast, we suggest that cystine A20−B19, involving sites distant in the polypeptide sequence, is favored because of intrinsic long-range structural propensities in the reduced polypeptide. We thus envisage that the [A20−B19] species represents the first "structural" intermediate, i.e., a species containing a stable partial fold with native-like long-range contacts. This partial fold can form in the absence or presence of cystine A6−A11, here regarded as peripheral to the initial logic of the conformational search. Our model is consistent with the observation that pairwise serine substitution of Cys^{A20} and Cys^{B19} (but not that of Cys^{A6} and Cys^{A11}) precludes biosynthetic expression of proinsulin analogues in yeast (*59*).

Insulin-like growth factor I (IGF-I), a single-chain protein homologous to proinsulin, refolds to native and non-native disulfide isomers (*8*−*10*). The non-native isomer (designated IGF-swap) contains pairings A7−A11, A6−B7, and A20−B19 (using insulin nomenclature; residues 6−48, 47−52, and 18−61 in IGF-I). The two products exhibit similar thermodynamic stabilities (*9*). Formation of the non-native isomer in vivo is avoided by coexpression of specific IGF-1 binding proteins: formation of a specific complex shifts the equilibrium to favor the native pairing scheme (*10*). As in studies of insulin precursors (*15*), refolding of IGF-I proceeds via a well-defined set of disulfide intermediates (*13*, *17*). The first populated intermediate contains cystine 18−61 (corresponding to cystine A20−B19 in insulin; *8*, *9*). Engineered models of this and subsequent two-disulfide intermediates suggest stepwise stabilization of structure with successive disulfide bond formation (*15*, *35*, *46*). "Strain" of cystine 47−52 in native IGF-I (corresponding to cystine A6−A11 in insulin) is proposed to favor disulfide rearrangement to the swapped isomer containing cystine 48−52 (*12*). Such strain rationalizes the failure to detect during IGF-I refolding the accumulation of a single-disulfide species (i.e., corresponding to insulin species [A6−A11]). The structural basis of strain in IGF-I has not been defined. Like the corresponding disulfide isomer of human insulin (*71*), IGF-swap shares some but not all of the structural features of native IGF-I (*72*). The swapped disulfide pairing scheme corresponds to a possible kinetic trap in the folding of proinsulin or insulin (*71*). It is not understood why the energy landscape of IGF-I contains two minima whereas that of proinsulin contains a single ground state. The strain hypothesis in IGF-I does not account for the marked instability of the "swapped" isomer of human insulin.

Concluding Remarks. This study has focused on a two-disulfide analogue of human insulin corresponding to a late folding intermediate. The results are of interest from the complementary perspectives of structure, function, and folding. The analogue retains a native-like B subdomain with asymmetric destabilization of the A chain. Although such a partial fold would be expected to exhibit impaired function, the analogue exhibits an extraordinary decrease in receptor affinity (10^5-fold), larger than what seems to be compatible with straightforward restoration of an active structure by induced fit. We propose that the exposed A7−B7 disulfide bridge not only stabilizes the hormone's global structure but also enters a hydrophobic milieu on binding of the hormone to the insulin receptor. This milieu may be either within the bound hormone or at the hormone−receptor interface. Any direct contacts would extend insulin's hydrophobic receptor-binding surface (*3*, *60*−*62*). That the homologous analogue of IGF-I retains higher activity (*12*, *35*) suggests a marked difference in either the structure or mode of receptor binding.

Structures of disulfide analogues of insulin and IGF-I exhibit a hierarchical family of partial folds. Whereas classical studies of protein folding focused on such intermediates and intervening barriers within predetermined pathways (Figure 9A), the "new view" envisages myriad trajectories along a funnel-like free energy landscape (Figure 9B; *73*, *74*). Discrete intermediates are not necessary and,

[8] Interpretation of the BPTI disulfide pathway (*47*) has engendered controversy first because of technical reassessment focused on the role of non-native disulfide bridges (*84*) and subsequently by its peripheral relationship to the energy landscape paradigm (new view; *75*, *76*, *85*). Because certain one-disulfide analogues exhibit native-like structures (*28*−*30*, *86*), the BPTI disulfide pathway primarily reflects the existence of kinetic barriers en route to the native state (*27*, *87*) and the need for error correction via protein unfolding (*26*, *88*−*90*). Native structure in a two-disulfide analogue has been demonstrated by X-ray crystallography (*91*). Partially folded BPTI intermediates have also been characterized (*92*−*94*).

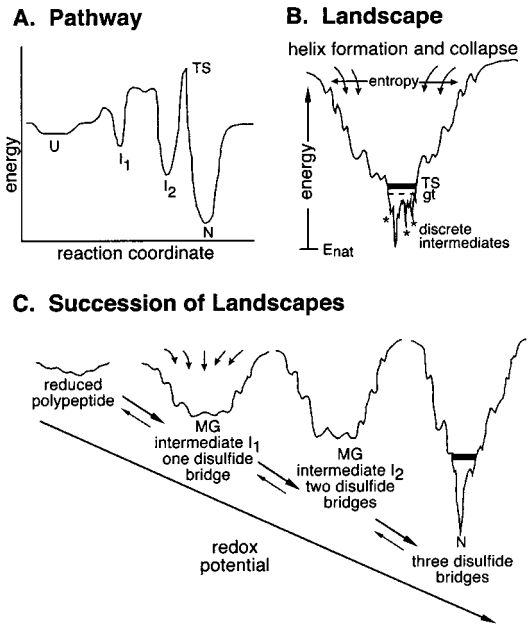

FIGURE 9: Synthesis of classical pathway and landscape paradigms (*74*−*78*). (A) A classical kinetic pathway is indicated in schematic form in relation to a reaction coordinate. TS represents the transition state. U and N represent unfolded and native states, and I_1 and I_2 classical intermediate states. (B) Funnel model of the free energy landscape in the new view of protein folding. Discrete intermediates are relegated to incidental features near the global minimum, peripheral to the major mechanisms involved in the folding chain's conformational search. (C) Proposed synthesis in which stepwise oxidative folding of proinsulin and related proteins is viewed as a pathway of successive energy landscapes with redox-sensitive depth and topography. Because introduction of cross-links alters chain entropy at each step, the physics of folding chains with zero to three disulfide bridges differs in character in accord with experimental observation of hierarchical stabilization of structural subdomains. Classical intermediates correspond to ensembles of partial folds on an intermediate landscape. Such intermediate landscapes are envisaged as integral (rather than incidental) to the proposed folding mechanism. Mg designates molten globule.

when populated, may merely represent off-pathway kinetic traps. We revisit the phenomenology of oxidative protein folding from the perspective of energy landscapes. New and classical viewpoints may be reconciled (*75*) by associating individual disulfide pairing schemes with distinct redox-dependent landscapes. Because a disulfide bridge alters the connectivity of the polypeptide chain, each oxidative intermediate (in the absence of disulfide exchange) may be viewed as exploring a distinct landscape. Further, the instability of the insulin motif and its hierarchy of partial folds imply large changes in landscape topography. Accordingly, we imagine that the folding proinsulin chain is engaged in a series of conformational searches along a succession of redox-dependent energy landscapes (Figure 9C). Formation of successive disulfide bridges represents a jump from one hypersurface to another. A particular pairing scheme may thus be used to label a landscape rather than a structure. The disulfide pathway of insulin-like proteins may thus be viewed as a succession of conformational searches by ensembles of progressive partial folds. This perspective, oxidative folding as a search along a hierarchy of landscapes, depends on and is unmasked by the instability of the insulin motif.

ACKNOWLEDGMENT

We thank Y. M. Feng for discussion and communication of results prior to publication; R. Chance, M. DeFelipis, and B. H. Frank (Eli Lilly and Co., Indianapolis, IN) for gift of human insulin and advice; K. Polonksy for support through the University of Chicago Diabetes Research and Training Center; a reviewer for valuable suggestions regarding the R- and T-state structures of insulin; and G. G. Dodson, M. Karplus, S. Rice, D. F. Steiner, M. Zhao, and the late H. S. Tager for discussion. M.A.W. thanks A. A. Kossickoff for his encouragement to continue these studies in Cleveland. NMR spectra were obtained at the Biomolecular NMR Facility at The University of Chicago and the Cleveland Center for Structural Biology.

SUPPORTING INFORMATION AVAILABLE

Five figures and three tables providing additional structural models and NMR data. This material is available free of charge via the Internet at http://pubs.acs.org.

REFERENCES

1. Steiner, D. F., and Chan, S. J. (1988) An overview of insulin evolution, *Horm. Metab. Res. 20*, 443−444.
2. Dodson, G., and Steiner, D. (1998) The role of assembly in insulin's biosynthesis, *Curr. Opin. Struct. Biol. 8*, 189−194.
3. Baker, E. N., Blundell, T. L., Cutfield, J. F., Cutfield, S. M., Dodson, E. J., Dodson, G. G., Hodgkin, D. M., Hubbard, R. E., Isaacs, N. W., and Reynolds, C. D. (1988) The structure of 2Zn pig insulin crystals at 1.5 Å resolution, *Philos. Trans. Royal Soc. London Ser. 319*, 369−456.
4. Katsoyannis, P. G., and Tometsko, A. (1966) Insulin synthesis by recombination of A and B chains: a highly efficient method, *Proc. Natl. Acad. Sci. U.S.A. 55*, 1554−1561.
5. Sieber, P. S., Eisler, K., Kamber, B., Riniker, B., Rittel, W., Marki, F., and deGasparo, M. (1978) Synthesis and biological activity of two disulphide bond isomers of human insulin: [A7-A11, A6-B7-cystine] and [A6-A7, A11-B7-cystine] insulin (human), *Hoppe-Seyler's Z. Physiol. Chem. 359*, 113−123.
6. Chance, R. E., Hoffman, J. A., Kroeff, E. P., Johnson, M. G., Schirmer, W. E., and Bormer, W. W. (1981) in *Peptides: Synthesis, Structure and Function; Proceedings of the Seventh American Peptide Symposium* (Rich, D. H., and Gross, E., Eds.) pp 721−728, Pierce Chemical Co., Rockford, IL.
7. Tang, J. G., and Tsou, C. L. (1990) The insulin A and B chains contain structural information for the formation of the native molecule. Studies with protein disulphide isomerase, *Biochem. J. 268*, 429−435.
8. Hober, S., Forsberg, G., Palm, G., Hartmanis, M., and Nilsson, B. (1992) Disulfide exchange folding of insulin-like growth factor I, *Biochemistry 31*, 1749−1756.
9. Miller, J. A., Narhi, L. O., Hua, Q. X., Rosenfeld, R., Arakawa, T., Rohde, M., Prestrelski, S., Lauren, S., Stoney, K. S., Tsai, L., et al. (1993) Oxidative refolding of insulin-like growth factor 1 yields two products of similar thermodynamic stability: a bifurcating protein-folding pathway, *Biochemistry 32*, 5203−5213.
10. Hober, S., Hansson, A., Uhlen, M., and Nilsson, B. (1994) Folding of insulin-like growth factor I is thermodynamically controlled by insulin-like growth factor binding protein, *Biochemistry 33*, 6758−6761.
11. Rosenfeld, R. D., Miller, J. A., Narhi, L. O., Hawkins, N., Katta, V., Lauren, S., Weiss, M. A., and Arakawa, T. (1997) Putative folding pathway of insulin-like growth factor-I, *Arch. Biochem. Biophys. 342*, 298−305.
12. Hober, S., Uhlen, M., and Nilsson, B. (1997) Disulfide exchange folding of disulfide mutants of insulin-like growth factor I in vitro, *Biochemistry 36*, 4616−4622.
13. Yang, Y., Wu, J., and Watson, J. T. (1999) Probing the folding pathways of long R(3) insulin-like growth factor-I (LR(3)-

IGF-I) and IGF-I via capture and identification of disulfide intermediates by cyanylation methodology and mass spectrometry, *J. Biol. Chem. 274*, 37598−37604.
14. Yuan, Y., Wang, Z. H., and Tang, J. G. (1999) Intra-A chain disulphide bond forms first during insulin precursor folding, *Biochem. J. 343* (Part 1), 139−144.
15. Qiao, Z. S., Guo, Z. Y., and Feng, Y. M. (2001) Putative disulfide-forming pathway of porcine insulin precursor during its refolding in vitro, *Biochemistry 40*, 2662−2668.
16. Videnov, G., Buttner, K., Casaretto, M., Fohles, J., Gattner, H. G., Stoev, S., and Brandenburg, D. (1990) Studies on the total synthesis of an A7,B7-dicarbainsulin. III. Assembly of segments and generation of biological activity, *Biol. Chem. Hoppe-Seyler 371*, 1057−1066.
17. Milner, S. J., Carver, J. A., Ballard, F. J., and Francis, G. L. (1999) Probing the disulfide folding pathway of insulin-like growth factor-I, *Biotechnol. Bioeng. 62*, 693−703.
18. Steiner, D. F. (1967) Evidence for a precursor in the biosynthesis of insulin, *Trans. N.Y. Acad. Sci. 30*, 60−68.
19. Markussen, J., Jorgensen, K. H., Sorensen, A. R., and Thim, L. (1985) Single chain des-(B30) insulin. Intramolecular crosslinking of insulin by trypsin catalyzed transpeptidation, *Int. J. Pept. Protein Res. 26*, 70−77.
20. Brems, D. N., Alter, L. A., Beckage, M. J., Chance, R. E., DiMarchi, R. D., Green, L. K., Long, H. B., Pekar, A. H., Shields, J. E., and Frank, B. H. (1992) Altering the association properties of insulin by amino acid replacement, *Protein Eng. 5*, 527−533.
21. Zhang, Y., Hu, H., Cai, R., Feng, Y., Zhu, S., He, Q., Tang, Y., Xu, M., Xu, Y., Zhang, X., Liu, B., and Liang, Z. (1996) Secretory expression of a single-chain insulin precursor in yeast and its conversion into human insulin, *Sci. China, Ser. C: Life Sci. 39*, 211−217.
22. Heath, W. F., Belagaje, R. M., Brooke, G. S., Chance, R. E., Hoffmann, J. A., Long, H. B., Reams, S. G., Roundtree, C., Shaw, W. N., Slieker, L. J., et al. (1992) (A-C-B) human proinsulin, a novel insulin agonist and intermediate in the synthesis of biosynthetic human insulin, *J. Biol. Chem. 267*, 419−425.
23. Hu, S. Q., Burke, G. T., Schwartz, G. P., Ferderigos, N., Ross, J. B., and Katsoyannis, P. G. (1993) Steric requirements at position B12 for high biological activity in insulin, *Biochemistry 32*, 2631−2635.
24. Oas, T. G., and Kim, P. S. (1988) A peptide model of a protein folding intermediate, *Nature 336*, 42−48.
25. Baldwin, R. L., and Rose, G. D. (1999) Is protein folding hierarchic? II. Folding intermediates and transition states, *Trends Biochem. Sci. 24*, 77−83 [erratum in *Trends Biochem. Sci. 24* (5), 185].
26. Weissman, J. S., and Kim, P. S. (1995) A kinetic explanation for the rearrangement pathway of BPTI folding, *Nat. Struct. Biol. 2*, 1123−1130.
27. Darby, N. J., Morin, P. E., Talbo, G., and Creighton, T. E. (1995) Refolding of bovine pancreatic trypsin inhibitor via non-native disulphide intermediates, *J. Mol. Biol. 249*, 463−477.
28. States, D. J., Creighton, T. E., Dobson, C. M., and Karplus, M. (1987) Conformations of intermediates in the folding of the pancreatic trypsin inhibitor, *J. Mol. Biol. 195*, 731−739.
29. van Mierlo, C. P., Darby, N. J., Neuhaus, D., and Creighton, T. E. (1991) Two-dimensional ^{1}H nuclear magnetic resonance study of the (5−55) single-disulphide folding intermediate of bovine pancreatic trypsin inhibitor, *J. Mol. Biol. 222*, 373−390.
30. Staley, J. P., and Kim, P. S. (1992) Complete folding of bovine pancreatic trypsin inhibitor with only a single disulfide bond, *Proc. Natl. Acad. Sci. U.S.A. 89*, 1519−1523.
31. Weiss, M. A., Hua, Q. X., Lynch, C. S., Frank, B. H., and Shoelson, S. E. (1991) Heteronuclear 2D NMR studies of an engineered insulin monomer: assignment and characterization of the receptor-binding surface by selective ^{2}H and ^{13}C labeling with application to protein design, *Biochemistry 30*, 7373−7389.
32. DiMarchi, R. D., Mayer, J. P., Fan, L., Brems, D. N., Frank, B. H., Green, J. K., Hoffman, J. A., Howey, D. C., Long, H. B., Shaw, W. N., Shields, J. E., Slieker, L. J., Su, K. S. E., Sundell, K. L., and Chance, R. E. (1992) in *Peptides: Proceedings of the Twelfth American Peptide Symposium* (Smith, J. A., and Rivier, J. E., Eds.) pp 26−28, ESCOM Science Publishers, Leiden, The Netherlands.
33. Shoelson, S. E., Lu, Z. X., Parlautan, L., Lynch, C. S., and Weiss, M. A. (1992) Mutations at the dimer, hexamer, and receptor-binding, surfaces of insulin independently affect insulin-insulin and insulin-receptor interactions, *Biochemistry 31*, 1757−1767.
34. Hua, Q. X., Hu, S. Q., Frank, B. H., Jia, W., Chu, Y. C., Wang, S. H., Burke, G. T., Katsoyannis, P. G., and Weiss, M. A. (1996) Mapping the functional surface of insulin by design: structure and function of a novel A-chain analogue, *J. Mol. Biol. 264*, 390−403.
35. Narhi, L. O., Hua, Q. X., Arakawa, T., Fox, G. M., Tsai, L., Rosenfeld, R., Holst, P., Miller, J. A., and Weiss, M. A. (1993) Role of native disulfide bonds in the structure and activity of insulin-like growth factor 1: genetic models of protein-folding intermediates, *Biochemistry 32*, 5214−5221.
36. Barany, G., and Merrifield, R. B. (1980) in *The Peptides* (Gross, E., and Meienhofer, J., Eds.) pp 3−284, Academic Press, New York.
37. Pittman, I., Nakagawa, S. H., Tager, H. S., and Steiner, D. F. (1997) Maintenance of B-chain beta-turn in [Gly^{B24}] insulin mutants: a steady-state fluorescence anisotrophy study, *Biochemistry 36*, 3430−3437.
38. Hua, Q. X., and Weiss, M. A. (1991) Comparative 2D NMR studies of human insulin and *des*-pentapeptide insulin: sequential resonance assignment and implications for protein dynamics and receptor recognition, *Biochemistry 30*, 5505−5515.
39. Hua, Q. X., Shoelson, S. E., Kochoyan, M., and Weiss, M. A. (1991) Receptor binding redefined by a structural switch in a mutant human insulin, *Nature 354*, 238−241.
40. Sosnick, T. R., Fang, X., and Shelton, V. M. (2000) Application of circular dichroism to study RNA folding transitions, *Methods Enzymol. 317*, 393−409.
41. Pace, C. N., and Shaw, K. L. (2000) Linear extrapolation method of analyzing solvent denaturation curves, *Proteins* (Suppl. 4), 1−7.
42. Luo, Y., and Baldwin, R. L. (2001) How Ala→Gly mutations in different helices affect the stability of the apomyoglobin molten globule, *Biochemistry 40*, 5283−5289.
43. Weiss, M. A., Hua, Q.-X., Jia, W., Chu, Y.-C., Wang, R.-Y., and Katsoyannis, P. G. (2000) Hierarchiacal protein "undesign": insulin's intrachain disulfide bridge tethers a recognition α-helix, *Biochemistry 39*, 15429−15440.
44. Courtenay, E. S., Capp, M. W., Saecker, R. M., and Record, M. T. J. (2000) Thermodynamic analysis of interactions between denaturants and protein surface exposed on unfolding: interpretation of urea and guanidinium chloride m-values and their correlation with changes in accessible surface area (ASA) using preferential interaction coefficients and the local-bulk domain model, *Proteins* (Suppl. 4), 72−85.
45. Weiss, M. A., Eliason, J. L., and States, D. J. (1984) Dynamic filtering by two-dimensional ^{1}H NMR with application to phage lambda repressor, *Proc. Natl. Acad. Sci. U.S.A. 81*, 6019−6023.
46. Hua, Q. X., Narhi, L., Jia, W., Arakawa, T., Rosenfeld, R., Hawkins, N., Miller, J. A., and Weiss, M. A. (1996) Native and non-native structure in a protein-folding intermediate: spectroscopic studies of partially reduced IGF-I and an engineered alanine model, *J. Mol. Biol. 259*, 297−313.
47. Goldenberg, D. P. (1992) Native and non-native intermediates in the BPTI folding pathway, *Trends Biochem. Sci. 17*, 257−261 [erratum in *Trends Biochem. Sci. 17* (9), 339].
48. Ikeguchi, M., Sugai, S., Fujino, M., Sugawara, T., and Kuwajima, K. (1992) Contribution of the 6−120 disulfide bond of α-lactalbumin to the stabilities of its native and molten globule states, *Biochemistry 31*, 12695−12700.

49. Ewbank, J. J., and Creighton, T. E. (1993) Structural characterization of the disulfide folding intermediates of bovine α-lactalbumin, *Biochemistry 32*, 3694−3707.
50. Peng, Z. Y., Wu, L. C., Schulman, B. A., and Kim, P. S. (1995) Does the molten globule have a native-like tertiary fold? *Philos. Trans. R. Soc. London, Ser. B 348*, 43−47.
51. Balbach, J., Forge, V., van Nuland, N. A., Winder, S. L., Hore, P. J., and Dobson, C. M. (1995) Following protein folding in real time using NMR spectroscopy, *Nat. Struct. Biol. 2*, 865−870.
52. Redfield, C., Schulman, B. A., Milhollen, M. A., Kim, P. S., and Dobson, C. M. (1999) α-Lactalbumin forms a compact molten globule in the absence of disulfide bonds, *Nat. Struct. Biol. 6*, 948−952.
53. Talluri, S., Rothwarf, D. M., and Scheraga, H. A. (1994) Structural characterization of a three-disulfide intermediate of ribonuclease A involved in both the folding and unfolding pathways, *Biochemistry 33*, 10437−10449.
54. Xu, X., and Scheraga, H. A. (1998) Kinetic folding pathway of a three-disulfide mutant of bovine pancreatic ribonuclease A missing the [40−95] disulfide bond, *Biochemistry 37*, 7561−7571.
55. Welker, E., Narayan, M., Volles, M. J., and Scheraga, H. A. (1999) Two new structured intermediates in the oxidative folding of RNase A, *FEBS Lett. 460*, 477−479.
56. Volles, M. J., Xu, X., and Scheraga, H. A. (1999) Distribution of disulfide bonds in the two-disulfide intermediates in the regeneration of bovine pancreatic ribonuclease A: further insights into the folding process, *Biochemistry 38*, 7284−7293.
57. Chakrabartty, A., Kortemme, T., and Baldwin, R. L. (1994) Helix propensities of the amino acids measured in alanine-based peptides without helix-stabilizing side-chain interactions, *Protein Sci. 3*, 843−852.
58. Karplus, P. A. (1997) Hydrophobicity regained, *Protein Sci. 6*, 1302−1307.
59. Guo, Z.-Y., and Feng, Y.-M. (2001) Effects of cysteine to serine substitutions in the two intra-A-chain disulfide bonds of insulin, *Biol. Chem. Hoppe-Seyler 382*, 443−448.
60. Pullen, R. A., Lindsay, D. G., Wood, S. P., Tickle, I. J., Blundell, T. L., Wollmer, A., Krail, G., Brandenburg, D., Zahn, H., Gliemann, J., and Gammeltoft, S. (1976) Receptor-binding region of insulin, *Nature 259*, 369−373.
61. De Meyts, P., Van Obberghen, E., and Roth, J. (1978) Mapping of the residues responsible for the negative cooperativity of the receptor-binding region of insulin, *Nature 273*, 504−509.
62. Liang, D. C., Chang, W. R., and Wan, Z. L. (1994) A proposed interaction model of the insulin molecule with its receptor, *Biophys. Chem. 50*, 63−71.
63. Bentley, G., Dodson, E., Dodson, G., Hodgkin, D., and Mercola, D. (1976) Structure of insulin in 4-zinc insulin, *Nature 261*, 166−168.
64. Derewenda, U., Derewenda, Z., Dodson, E. J., Dodson, G. G., Reynolds, C. D., Smith, G. D., Sparks, C., and Swenson, D. (1989) Phenol stabilizes more helix in a new symmetrical zinc insulin hexamer, *Nature 338*, 594−596.
65. Roy, M., Brader, M. L., Lee, R. W., Kaarsholm, N. C., Hansen, J. F., and Dunn, M. F. (1989) Spectroscopic signatures of the T to R conformational transition in the insulin hexamer, *J. Biol. Chem. 264*, 19081−19085.
66. Brader, M. L., and Dunn, M. F. (1991) Insulin hexamers: new conformations and applications, *Trends Biochem. Sci. 16*, 341−345.
67. De Meyts, P. (1994) The structural basis of insulin and insulin-like growth factor-I receptor binding and negative cooperativity, and its relevance to mitogenic versus metabolic signalling, *Diabetologia 37* (Suppl. 2), S135−S148.
68. Hodgson, D. R., May, F. E., and Westley, B. R. (1995) Mutations at positions 11 and 60 of insulin-like growth factor 1 reveal differences between its interactions with the type I insulin-like-growth-factor receptor and the insulin receptor, *Eur. J. Biochem. 233*, 299−309.
69. Gill, R., Wallach, B., Verma, C., Urso, B., De Wolf, E., Grotzinger, J., Murray-Rust, J., Pitts, J., Wollmer, A., De Meyts, P., and Wood, S. (1996) Engineering the C-region of human insulin-like growth factor-1: implications for receptor binding, *Protein Eng. 9*, 1011−1019.
70. Gill, R., Verma, C., Wallach, B., Urso, B., Pitts, J., Wollmer, A., De Meyts, P., and Wood, S. (1999) Modelling of the disulphide-swapped isomer of human insulin-like growth factor-1: implications for receptor binding, *Protein Eng. 12*, 297−303.
71. Hua, Q. X., Gozani, S. N., Chance, R. E., Hoffmann, J. A., Frank, B. H., and Weiss, M. A. (1995) Structure of a protein in a kinetic trap, *Nat. Struct. Biol. 2*, 129−138.
72. Sato, A., Koyama, S., Yamada, H., Suzuki, S., Tamura, K., Kobayashi, M., Niwa, M., Yasuda, T., Kyogoku, Y., and Kobayashi, Y. (2000) Three-dimensional solution structure of a disulfide bond isomer of the human insulin-like growth factor-I, *J. Pept. Res. 56*, 218−230.
73. Rock, F. L., Li, X., Chong, P., Ida, N., and Klein, M. (1994) Roles of disulfide bonds in recombinant human interleukin 6 conformation, *Biochemistry 33*, 5146−5154.
74. Rumbley, J., Hoang, L., Mayne, L., and Englander, S. W. (2001) An amino acid code for protein folding, *Proc. Natl. Acad. Sci. U.S.A. 98*, 105−112.
75. Lazaridis, T., and Karplus, M. (1997) "New view" of protein folding reconciled with the old through multiple unfolding simulations, *Science 278*, 1928−1931.
76. Baldwin, R. L. (1995) The nature of protein folding pathways: the classical versus the new view, *J. Biomol. NMR 5*, 103−109.
77. Onuchic, J. N., Luthey-Schulten, Z., and Wolynes, P. G. (1997) Theory of protein folding: the energy landscape perspective, *Annu. Rev. Phys. Chem. 48*, 545−600.
78. Pande, V. S., Grosberg, A., Tanaka, T., and Rokhsar, D. S. (1998) Pathways for protein folding: is a new view needed? *Curr. Opin. Struct. Biol. 8*, 68−79.
79. Olsen, H. B., Ludvigsen, S., and Kaarsholm, N. C. (1996) Solution structure of an engineered insulin monomer at neutral pH, *Biochemistry 35*, 8836−8845.
80. Brandenburg, D., Gattner, H. G., Weiner, M., Herbertz, L., Zanh, H., and Wollmer, A. (1971) Structure function studies with derivatives and analogs of insulin and its chains, *Int. Congr. Ser. 231*, 363−376.
81. Busse, W. D., and Gattner, H. G. (1973) Selective cleavage of one disulfide bond in insulin: preparation and properties of insulin A7-B7-di-S-sulfonate, *Hoppe-Seylers Z. Physiol. Chem. 354*, 147−155.
82. Marki, F., de Gasparo, M., Eisler, K., Kamber, B., Riniker, B., Rittel, W., and Sieber, P. (1979) Synthesis and biological activity of seventeen analogues of human insulin, *Hoppe-Seyler's Z. Physiol. Chem. 360*, 1619−1632.
83. Dai, Y., and Tang, J. G. (1996) Characteristic, activity and conformational studies of [A6-Ser, A11- Ser]-insulin, *Biochim. Biophys. Acta 1296*, 63−68.
84. Weissman, J. S., and Kim, P. S. (1991) Reexamination of the folding of BPTI: predominance of native intermediates, *Science 253*, 1386−1393.
85. Dill, K. A., and Chan, H. S. (1997) From Levinthal to pathways to funnels, *Nat. Struct. Biol. 4*, 10−19.
86. Dadlez, M., and Kim, P. S. (1995) A third native one-disulphide intermediate in the folding of bovine pancreatic trypsin inhibitor, *Nat. Struct. Biol. 2*, 674−679.
87. Darby, N. J., and Creighton, T. E. (1993) Dissecting the disulphide-coupled folding pathway of bovine pancreatic trypsin inhibitor. Forming the first disulphide bonds in analogues of the reduced protein, *J. Mol. Biol. 232*, 873−896.
88. Weissman, J. S., and Kim, P. S. (1992) Kinetic role of nonnative species in the folding of bovine pancreatic trypsin inhibitor, *Proc. Natl. Acad. Sci. U.S.A. 89*, 9900−9904.
89. Ferrer, M., Barany, G., and Woodward, C. (1995) Partially folded, molten globule and molten coil states of bovine pancreatic trypsin inhibitor, *Nat. Struct. Biol. 2*, 211−217.

90. Barbar, E., Hare, M., Daragan, V., Barany, G., and Woodward, C. (1998) Dynamics of the conformational ensemble of partially folded bovine pancreatic trypsin inhibitor, *Biochemistry 37*, 7822−7833.
91. Eigenbrot, C., Randal, M., and Kossiakoff, A. A. (1990) Structural effects induced by removal of a disulfide-bridge: the X-ray structure of the C30A/C51A mutant of basic pancreatic trypsin inhibitor at 1.6 Å, *Protein Eng. 3*, 591−598.
92. van Mierlo, C. P., Darby, N. J., Keeler, J., Neuhaus, D., and Creighton, T. E. (1993) Partially folded conformation of the (30−51) intermediate in the disulphide folding pathway of bovine pancreatic trypsin inhibitor. ^{1}H and ^{15}N resonance assignments and determination of backbone dynamics from ^{15}N relaxation measurements, *J. Mol. Biol. 229*, 1125−1146.
93. van Mierlo, C. P., Kemmink, J., Neuhaus, D., Darby, N. J., and Creighton, T. E. (1994) ^{1}H NMR analysis of the partly-folded non-native two-disulphide intermediates (30−51,5−14) and (30−51,5−38) in the folding pathway of bovine pancreatic trypsin inhibitor, *J. Mol. Biol. 235*, 1044−1061.
94. Creighton, T. E., Darby, N. J., and Kemmink, J. (1996) The roles of partly folded intermediates in protein folding, *FASEB J. 10*, 110−118.

BI011021O